Patterns of the Effect of the Temperature of Spark Plasma Sintering on the Microstructure of Thermoelectric Composites Based on the Matrix of Bi₂Te_{2,1}Se_{0,9}Bi₂ with Cobalt Inclusions

M. Zhezhu^{a, *}, A. E. Vasil'ev^b, and O. N. Ivanov^{a, b}

^a Belgorod State Technological University, Belgorod, 308012 Russia
^b Belgorod State University, Belgorod, 308015 Russia
*e-mail: marina_jeju@mail.ru
Received December 5, 2022; revised December 23, 2022; accepted February 27, 2023

Abstract—A study is performed of the effect the temperature of spark plasma sintering has on the formation of Co filler particles in the matrix of $Bi_2Te_{2.1}Se_{0.9}$. Core—shell filler particles (Co@CoTe₂) form in $Bi_2Te_{2.1}Se_{0.9} + 0.33$ Co (wt %) due to the high-temperature diffusion redistribution of atoms in the matrix and filler materials, and the chemical interaction between these materials. The fraction of CoTe₂ shells in the particles grows along with the temperature of sintering, while the fraction of the Co cores shrinks. This behavior is due to an increase in the diffusion coefficient of Co in the $Bi_2Te_{2.1}Se_{0.9}$ matrix as the temperature of sintering rises. The concentration profiles of the Co distribution of in the $Bi_2Te_{2.1}Se_{0.9}$ matrix, governed by diffusion, are described well by Fick's second law of diffusion from a limited source of a diffusing substance. The coefficient of Co diffusion grows along with the temperature of sintering in accordance with the Arrhenius law, and with an energy of activation of ~0.61 eV.

DOI: 10.3103/S1062873823701915

INTRODUCTION

The development of composites (nanocomposites) consisting of a thermoelectric matrix with inclusions of a filler that has different properties, sizes, and dimensions is an effective way of obtaining thermoelectric materials with enhanced thermoelectric Q-factors. The inclusions in such composites act as scattering centers for electrons that affect their electrical conductivity (σ) and phonons that affect their thermal conductivity (k). Thermoelectric composites consisting of a matrix based on bismuth telluride Bi₂Te₃ are now being studied, and magnetoactive elements M (M = Ni, Fe, Co) are used as inclusions in such composites [1, 2]. New physical mechanisms emerge because inclusion atoms have magnetic moments. These mechanisms have an additional effect on the transport properties (σ and k) of composites, allowing us to optimize these properties and raise the thermoelectrical Q-factor of the material [3, 4]. An essential feature of the microstructure of thermoelectric composites with magnetoactive inclusions is the formation of filler particles of core—shell type M@MTe₂ consisting of metallic cores M (filler material) and MTe₂ shells corresponding to the material that forms as a result of chemical interaction between the filler and matrix while preparing a composite. High-temperature diffusion redistribution of atoms of matrix and filler materials during the synthesis of a composite using the initial matrix and filler powders is the primary mechanism of the formation of "core—shell" particles. The formation of core—shell particles provides an additional possibility of influencing the degree of heterogeneity of the composite and its transport properties. It is the diffusion process that determines the formation of filler particles of the core—shell type in thermoelectric composites with magnetoactive inclusions, and the coefficient of diffusion depends on the temperature of the diffusion process. We may therefore conclude that the temperature of composite sintering determines such microstructure characteristics of composites as the filler size and the ratio of core and shell sizes.

The aim of this work was to establish the patterns of the effect spark plasma sintering has on the microstructure of core—shell inclusions formed in $\rm Bi_2Te_{2.1}Se_{0.9}$ (matrix) + 0.33 wt % Co (filler) thermoelectric composites.

EXPERIMENTAL

Bi₂Te_{2.1}Se_{0.9} (matrix) and Co (filler) initial powders were used to obtain the studied composites. The initial Bi₂Te_{2.1}Se_{0.9} sample was synthesized using the polyol technique. Bi₂O₃, NaHSeO₃, and TeO₂ (high purity grade) precursors were taken in a stoichiometric ratio

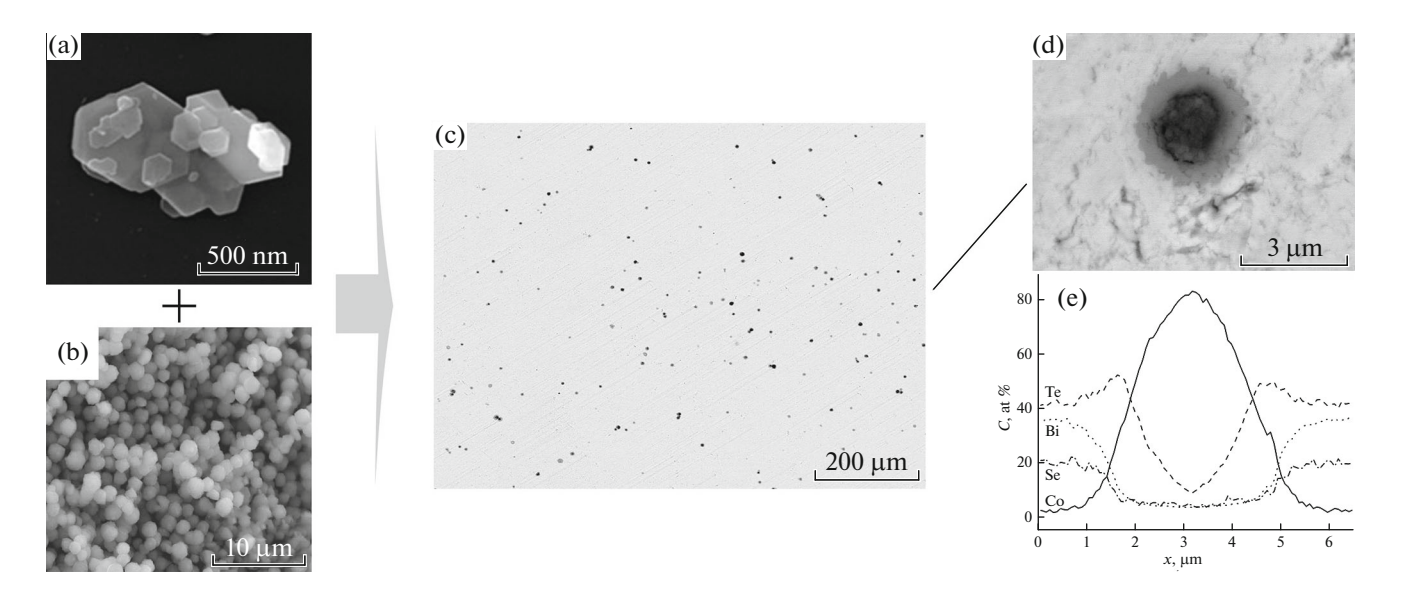


Fig. 1. (a, b) SEM images of particles of the initial $Bi_2Te_{2.1}Se_{0.9}$ and Co powders. (c, d) BSE images of a polished surface of composite $Bi_2Te_{2.1}Se_{0.9} + 0.33Co$ (wt %) sintered at 698 K and an individual inclusion. (e) Profiles of Bi, Te, Se, and Co distributions, collected along a line intersecting an inclusion.

and dissolved in ethylene glycol with an alkaline agent (KOH). The obtained solution was transferred to a round bottom flask and heated to the boiling point with constant stirring. After removing the water, the flask with the solution was hermetically sealed, covered with a reflux condenser, and kept for 4 h at a temperature of 458 K. After cooling to room temperature, the obtained suspension was centrifuged to separate Bi₂Te_{2.1}Se_{0.9} powder, which was then rinsed with isopropyl alcohol and acetone. The powder was dried for 12 h inside a vacuum cabinet at 373 K. The initial Co powder was obtained by reducing Co(NO₃)₂·6H₂O, which was mixed with the C₆H₈O₇ (citric acid) in a 1:1.5 ratio and dissolved in ethylene glycol with the addition of KOH alkali. The mixture was heated to 353 K with constant stirring to complete the dissolution of precursors. Reducing agent hydrazine hydrate N_2H_4 · H_2O was added slowly after cooling the obtained solution to room temperature. The reaction mixture was heated to 353 K and held for 6 h until the process of $Co^{2+} \rightarrow Co^0$ reduction was complete. The resulting powder was flushed with isopropyl alcohol and acetone until impurities were removed.

To obtain $\rm Bi_2Te_{2.1}Se_{0.9} + 0.33Co$ (wt %) composites, the initial powders of matrix and filler taken in a stoichiometric ratio were mixed thoroughly for 30 min using a planetary mill with agate balls and a rotating speed of 100 rpm. The final mixture was consolidated via spark plasma sintering (SPS) using an SPS-25/10 system (Thermal Technology, United States). Sintering was done for 5 min in a vacuum (2 × 10⁻² torr) at a pressure of 40 MPa and temperatures of sintering $T_{\rm s}$ of 598, 623, 648, 673, and 698 K. SPS yielded cylinders 20 mm in diameter and 15 mm tall.

The density of studied samples was determined according to Archimedes. X-ray diffraction (XRD) analysis on an Ultima IV (Rigaku, Japan) diffractometer with CuK_{α} radiation was used to determine the type and parameters of the crystal structure and phase composition of the initial powders and composites. Features of the composite's microstructure were studied via scanning electron microscopy (SEM) on a Nova NanoSEM 450 microscope (Thermo Fisher Scientific, United States). Energy dispersive X-ray spectroscopy (EDS) was used to obtain profiles of the distribution of elements in inclusions of the composite filler. SEM images were taken in the backscattered electron (BSE) mode to register the phase contrast associated with the formation and spatial distribution of different phases on the surfaces of samples.

RESULTS AND DISCUSSION

XRD showed the initial $Bi_2Te_{2.1}Se_{0.9}$ powder was single-phase and had the $R\overline{3}m$ hexagonal structure with lattice parameters of a=0.4304 nm and c=3.0000 nm. The $Bi_2Te_{2.1}Se_{0.9}$ powder consisted mainly of hexagonal plates ~500 nm in size and ~100 nm thick (Fig. 1a). The initial Co powder was single-phase and had the $P6_3/mmc$ hexagonal structure with lattice parameters of a=0.2507 nm and c=0.4069 nm. The Co powder consisted of spherical particles 1 μ m in size (Fig. 1b).

The density of our $Bi_2Te_{2.1}Se_{0.9} + 0.33Co$ (wt %) composites was ~7.62 g/cm³, which is in good agreement with the literature data [5] and virtually independent of T_s . The formation of desired matrix—filler microstructure of composites sintered at different

temperatures was confirmed by analyzing BSE images of polished composite surfaces. Different phases in the BSE images were visualized according to the degree of compositional contrast. The phase with the higher average atomic number reflected more electrons and produced brighter areas in the image. Figure 1c shows a typical BSE image of a composite with $T_s = 698$ K. The filler inclusions are shown as dark grey islands randomly distributed in the volume of a light grey matrix. According to results from elemental composition analysis, the matrix corresponds to the Bi₂Te_{2.1}Se_{0.9} compound. However, the composite's filler inclusions have both Co and a complex coreshell structure (Fig. 1d) corresponding to two different phases of the of core and shell materials. The existence of three phases (a matrix plus the core and shell materials of filler inclusions) was confirmed by XRD patterns collected on composites sintered at different temperatures (Fig. 2). We would expect the XRD patterns of $Bi_2Te_{2.1}Se_{0.9} + 0.33Co$ (wt %) composites to be a simple overlapping of XRD patterns corresponding to the Bi₂Te_{2.1}Se_{0.9} matrix and Co filler, and the phase with $R\overline{3}m$, crystal structure corresponding to $Bi_2Te_{2.1}Se_{0.9}$ does indeed predominate in the XRD patterns of all composites. Figure 2 presents the standard (given in the PDF database) XRD pattern of the Bi₂Te_{2.1}Se_{0.9} phase as a bar diagram. The content of Co is negligible, and its contribution to the composite XRD pattern cannot be reliably distinguished because the intensities of the diffraction peaks for the filler phase are comparable to the change in the background throughout the diffraction pattern. However, it is shown below that the Co phase was found in the filler inclusions of $Bi_2Te_{2.1}Se_{0.9} + 0.33Co$ (wt %) composites sintered at different temperatures. A new CoTe₂ phase was found in the XRD patterns of Bi₂Te_{2.1}Se_{0.9} + 0.33Co (wt %) composites. This phase had a *Pnam* rhombical structure with lattice cell parameters of a =0.5217, b = 0.6220, and c = 0.5426 nm. The magnified section of the XRD pattern in Fig. 2 confirms the formation of the CoTe₂ phase. The additional weak peak (230) typical of the CoTe₂ phase appears on the left slope of the main peak (015) of the Bi₂Te_{2.1}Se_{0.9} phase. The CoTe₂ phase apparently forms due to the chemical reaction $Co^0 + 2Te^{2-} \rightarrow CoTe_2$ between the filler and matrix materials, and the CoTe₂ phase forms as a shell surrounding a Co core (Fig. 1d). Similar results were obtained earlier on Bi₂Te₃ composites with Ni [6] and Fe [7] fillers. The formation of a new shell phase is based on the high-temperature diffuse redistribution of matrix and filler materials during the spark plasma sintering of the initial powders of the matrix and filler, and the process's corresponding coefficient of diffusion has to dramatically (exponentially) grow along with the temperature of sintering [8]. We would therefore expect that the Co atoms of inclusions penetrate deeper into the material of the Bi₂Te_{2.1}Se_{0.9} matrix

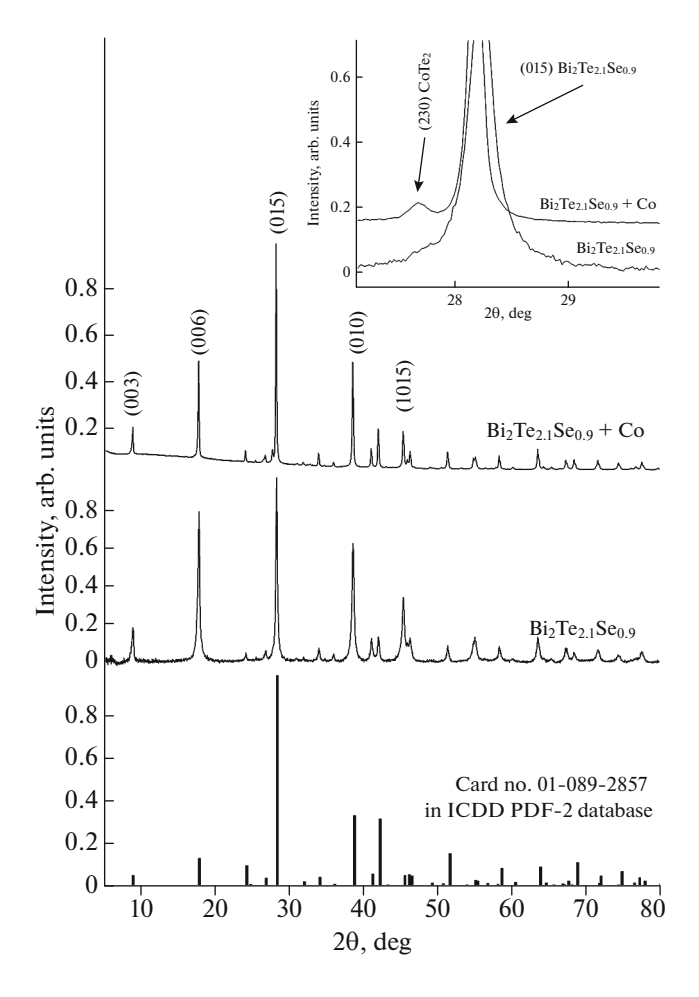


Fig. 2. XRD patterns of the $Bi_2Te_{2.1}Se_{0.9}$ matrix and the $Bi_2Te_{2.1}Se_{0.9} + 0.33Co$ (wt %) composite. The inset shows a magnified sector of the XRD patterns with the main peak (015) of the $Bi_2Te_{2.1}Se_{0.9}$ phase.

when the temperature of sintering is raised. As a consequence, the fraction of the CoTe₂ phase that forms as a shell based on the initial Co inclusions due to diffusion will grow and the fraction of the Co core will shrink. Finally, the ratio of core and shell fractions in Co@CoTe₂ inclusions depends on temperature of sintering T_s . These features of the effect the temperature of sintering has on the internal structure of Co@CoTe₂ inclusions were found in our experiment. Profiles of the Co distribution were collected along a line intersecting a Co@CoTe2 inclusion in order to obtain the corresponding concentration profiles. These profiles obtained by EDX are shown in Fig. 1e. They were used to obtain dependences $C/C_0 = f(x)$, where C_0 is the concentration of cobalt in the center of an inclusion and C = C(x) is the current concentration of Co depending on distance x from the center of the inclusion. Figure 3a shows $C/C_0 = f(x)$ concentration profiles obtained after sintering at (1) 598, (2) 623, and (3) 673 K. Co atoms penetrate deeper into the matrix when temperature of sintering T_s is raised. At the same

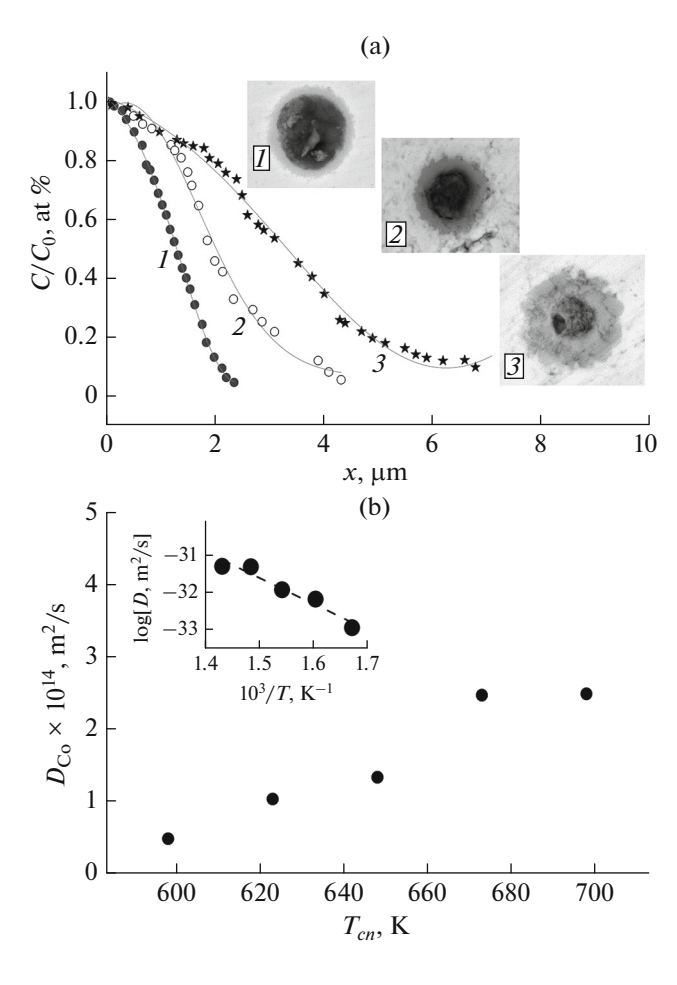


Fig. 3. (a) Concentration profiles of the distribution of Co in Co@CoTe₂ inclusions of Bi₂Te_{2.1}Se_{0.9} + 0.33Co (wt %) composites sintered at (1) 598, (2) 623, and (3) 673 K. A typical BSE image of Co@CoTe₂ particles is given for each profile. (b) Temperature dependence of the coefficient of Co diffusion in the Bi₂Te_{2.1}Se_{0.9} matrix. The inset shows dependence In $D_{Co} = f(1/T)$.

time, the internal structure of filler inclusions changes greatly, as is seen in the BSE images of typical filler inclusions at these temperatures. When $T_{\rm s}$ is raised, the shell fraction grows and the core fraction shrinks. In other words, the intensification of Co diffusion as a result of raising the spark plasma temperature of sintering increases the volume of the CoTe₂ phase.

It was established that $C/C_0 = f(x)$ dependences can be described by the expression

$$C(x,t) = \frac{Q_0}{2\sqrt{\pi Dt}} \exp\left(-\frac{x^2}{4Dt}\right),\tag{1}$$

where Q_0 is the initial amount of substance in a layer per unit area, t is the period of diffusion, and D is the coefficient of diffusion.

This equation is the solution to the equations of Fick's second law when dealing with a limited source

of diffusing matter [9]. The solid curves in Fig. 3a describe the experimental curves of the Co concentration profiles. Processing the experimental curves on the basis of expression (1) allowed us to estimate coefficient $D_{\rm Co}$ of cobalt diffusion in the Bi₂Te_{2.1}Se_{0.9} matrix. Dependence $D_{\rm Co}(T_{\rm s})$ is presented in Fig. 3b. We can see that $D_{\rm Co}$ grows along with the spark plasma temperature of sintering, behavior that is typical of diffusion processes. In addition, experimental dependence $D_{\rm Co}(T_{\rm s})$ can be described by the Arrhenius equations for thermally activated processes:

$$D = D_0 \exp\left[-E_a/(k_B T)\right],\tag{2}$$

where E_a is the energy of activation for diffusion, D_0 is a preexponential factor, and k_B is the Boltzmann constant.

As is shown in the inset in Fig. 3b, the $D_{\rm Co}(T_{\rm s})$ experimental dependence is linear in coordinates $\ln D_{\rm Co} - 1/T$. Characteristics of Co diffusion in the ${\rm Bi}_2{\rm Te}_{2.1}{\rm Se}_{0.9}$ matrix were obtained by processing experimental dependence $D_{\rm Co}(T_{\rm s})$: $E_{\rm a}=0.61$ eV and $D_0=7.2\times 10^{-10}$ m²/s. These values are typical of processes of atomic diffusion in solids. It should be noted that the values obtained for the coefficient of Co diffusion in ${\rm Bi}_2{\rm Te}_{2.1}{\rm Se}_{0.9}$ agree with the coefficients of diffusion of other elements (related or otherwise) in ${\rm Bi}_2{\rm Te}_3$ -compounds. For example, the coefficient of diffusion for Ni (a *d*-element of Fe subgroup along with Co) in bismuth telluride with electron-type conductivity was estimated to be 3.1×10^{-14} m²/s at a temperature of 500 K [10].

CONCLUSIONS

It was established that the temperature of spark plasma sintering greatly affects the microstructure of Co@CoTe₂ filler inclusions of the core—shell type that form in $Bi_2Te_{2.1}Se_{0.9} + 0.33Co$ wt % composite via chemical reaction $Co^0 + Te^{2-} \rightarrow CoTe_2$ between the matrix and filler materials. This reaction is initiated by the high-temperature diffuse redistribution of matrix and filler materials. At temperatures of 598, 623, 648, 673, and 698 K, the diffusion of Co in the $Bi_2Te_{2.1}Se_{0.9}$ matrix was found to grow along with the temperature of sintering. Such thermoactive behavior of the coefficient of diffusion increases the fraction of CoTe₂ shells and reduces the fraction of Co cores as the temperature of sintering rises. It should be noted that filler inclusions in thermoelectric composites act as centers of electron and phonon scattering that strongly affect the electrical and heat conductivities of the composite. The internal structure of Co@CoTe₂ inclusions can be deliberately changed by varying the temperature of sintering of Bi₂Te_{2.1}Se_{0.9}-Co composites, and filler inclusions can be obtained that ensure optimum values of the composite's electrical and heat conductivities.

ACKNOWLEDGMENTS

This work was performed on equipment at the Technologies and Materials resource center of Belgorod State University.

FUNDING

This work was supported by the RF Ministry of Science and Higher Education, project no. 0625-2020-0015.

CONFLICT OF INTEREST

The authors declare that they have no conflicts of interest.

REFERENCES

- Fortulan, R. and Yamini, S.A., *Materials*, 2021, vol. 14, no. 20, p. 6059.
- Zhao, W.LiuZ. Wei, P., et al., Nat. Nanotechnol., 2017, vol. 12, no. 1, p. 55.

- 3. Xing, L., Cui, W., Sang, X., et al., *J. Materiomics*, 2021, vol. 7, no. 5, p. 998.
- 4. Ma, S., Li, C., Wei, P., et al., *J. Mater. Chem. A*, 2020, vol. 8, no. 9, p. 4816.
- 5. Li, D., Zhang, J., Song, C.J., et al., *RSC Adv.*, 2015, vol. 5, no. 54, p. 43717.
- 6. Ivanov, O., Yaprintsev, M., Vasil'ev, A., et al., *Chin. J. Phys.*, 2022, vol. 77, p. 24.
- 7. Ivanov, O.N., Yapryntsev, M.N., Vasil'ev, A.E., et al., *Glass Ceram.*, 2022, vol. 78, p. 442.
- 8. Mehrer, H., *Diffusion in Solids: Fundamentals, Methods, Materials, Diffusion-Controlled Processes*, New York: Springer, 2007, p. 295.
- 9. Pavlov, P.V. and Khokhlov, A.F., *Fizika tverdogo tela* (Solid State Physics), Moscow: Lenand, 2015, p. 496.
- 10. Lan, Y.C., Wang, D.Z., Chen, G., et al., *Appl. Phys. Lett.*, 2008, vol. 92, p. 101910.

Translated by N. Saetova